Line competition in an intracavity diode-pumped Yb:KYW laser operating at 981 nm

François Balembois, Marc Castaing, Patrick Georges, Georges Thierry

Line competition in an intracavity diode-pumped Yb:KYW laser operating at 981 nm

François Balembois,[1,*] Marc Castaing,[1,2] Patrick Georges,[1] and Thierry Georges[2]

[1]*Laboratoire Charles Fabry de l'Institut d'Optique, CNRS, Université Paris-Sud, Campus Polytechnique, RD128, 91127 Palaiseau Cedex, France*
[2]*Oxxius SA, 4 Rue Louis de Broglie, F-22300 Lannion, France*
**Corresponding author: francois.balembois@institutoptique.fr*

Received September 9, 2010; revised October 22, 2010; accepted October 25, 2010; posted November 4, 2010 (Doc. ID 134771); published December 17, 2010

This paper proposes an analysis of a Yb:KYW laser emitting at 981 nm intracavity pumped by a $Nd:YVO_4$ laser operating at 914 nm. It gives some guidelines to optimize the laser performance. An output power of 1 W has been obtained at 981 nm for a pump power of 23 W at 808 nm. It presents a simple and original model to deal with the line competition between 981 nm and the other lines at 1000 and 1023 nm and explains how a temperature increase can promote the 981 nm laser emission. This approach could be useful for other lasers that are subject to line competition.

OCIS codes: 140.3480, 140.3580, 140.3430, 140.3615, 140.3530.

1. INTRODUCTION

Laser source developments around 980 nm based on ytterbium-doped materials are rising due to their wide range of applications. Moreover, the possibility of second harmonic generation (SHG) for a blue emission around 488 nm (corresponding to an argon-ionized transition) is another motivation for increasing the performance of this kind of source. Still, the three-level nature of the transition involves the use of very high pump intensity in order to avoid reabsorption losses at the lasing wavelength. This explains why the first laser systems emerging at 980 nm were fiber lasers [1,2], now demonstrating impressive output powers [3,4]. Indeed, the pump is confined throughout the propagation, enabling it to maintain a high level of population inversion and to limit the reabsorption losses. Moreover, the pump-signal overlap is enhanced in comparison with a direct diode pumping. However, this architecture suffers from two intrinsic limitations. First, the compacity is limited by the fiber length and its minimum radius of curvature. Second, cw intracavity SHG remains difficult to achieve with this kind of setup since the intracavity power is generally low in fiber lasers. Consequently, SHG with fiber lasers is generally carried out in an extracavity configuration. This leads to low efficiency and requires the use of very efficient nonlinear crystals (like ppLN or ppKTP) together with a high power at the fundamental wavelength 980 nm [5,6].

On the opposite hand, Yb-doped bulk crystals could be an alternative since they would offer the possibility of intracavity SHG and microchip integration. However, the direct diode pumping of crystalline three-level laser media remains difficult due to the bad spatial beam quality of high-power laser diodes. The intracavity pumping configuration represents one way to solve this problem as demonstrated in a Yb:S-FAP crystal [7]. Nevertheless, two problems appear with Yb:S-FAP. First, the emission wavelength is slightly red shifted with respect to the 976 nm operation required to approach the argon laser line after SHG. Moreover, this crystal is not commercially available. Closer to the required wavelength and more widely used are the ytterbium-doped tungstate crystals family, such as $Yb:KY(WO_4)_2$ (Yb:KYW) or $Yb:KGd(WO_4)_2$ (Yb:KGW). These crystals exhibit a strong emission line at 981 nm. Previously demonstrated under Ti:sapphire pumping [8], the first laser emission with Yb:KYW at 981 nm was achieved in 2009 [9] with an intracavity pumping configuration. A similar experiment was carried out later [10] demonstrating around 100 mW at 490.5 nm by SHG.

Through these publications, it appears that the laser design is not obvious. Indeed, the emission spectrum of Yb-doped tungstate is continuous between 981 and 1040 nm with peaks at 981, 1000, 1023, and 1040 nm [11], following the crystal orientation. As opposed to Yb:S-FAP [12], strong gain competition will occur between the 981 nm line and the other transitions. Moreover, the design of an intracavity-pumped laser requires adjusting the absorption carefully: if the absorption at the pump wavelength is too high, the threshold of the pump laser will increase, reducing the efficiency of the pump laser. Conversely if the absorption is too low, the output at 981 nm will be reduced.

The purpose of this paper is to give a theoretical analysis in order to design a Yb:tungstate laser at 981 nm with intracavity pumping at 914 nm by a $Nd:YVO_4$ laser. We also explain how to manage the line competition. This work is based on experimental results reported in [9] and a theoretical approach based on gain calculations. In Section 2, we explain how to choose the tungstate crystal: Yb:KYW or Yb:KGW. Section 3 deals with the absorption of the tungstate crystal, taking the intracavity pumping scheme into account. Section 4 explains how to adjust the transmission of the mirrors to avoid the line competition and promote laser emission at 981 nm. Finally, we investigate the temperature effect on the line competition between the 981 and 1000 nm transitions.

2. CHOICE OF THE Yb-DOPED TUNGSTATE CRYSTAL

The most widely used and commercially available tungstate crystals are Yb:KGW and Yb:KYW. Their properties are

relatively similar [13–15], and it is difficult to know which is the best for a laser emission at 981 nm. Table 1 gives the main properties to be considered for laser operation at 981 nm. The cross sections are from [13,14] and the lifetimes are from [15]. One should note that different values are given for the lifetimes : from 300 [16] to 600 μs [17].

The effective emission cross section is higher for Yb:KGW, whereas the effective absorption cross sections and the lifetimes are similar. One would thus be inclined to choose Yb:KGW over Yb:KYW. However, one has to take the line competition into account between 981 nm and the closest peak after 981 nm corresponding to 1000 nm for Yb:KYW and 997 nm for Yb:KGW (Fig. 1).

To investigate this problem, we consider the gain cross section σ_g:

$$\sigma_g = (\sigma_{\mathrm{el}} + \sigma_{\mathrm{al}}) \cdot x - \sigma_{\mathrm{al}}, \tag{1}$$

where σ_{el} and σ_{al} are the effective emission cross section and the effective absorption cross section at the considered laser wavelength, x is the ratio of the upper-level population density n_2 to the total density of Yb ions $n_t : x = n_2/n_t$. To reach the transparency at 981 nm (meaning a gain coefficient equal to zero), x needs to be 0.44 for Yb:KGW and 0.46 for Yb:KYW. This value is denoted x_{tr}. For this population inversion ratio, we calculate the gain cross section at 1000 nm in Yb:KYW and 997 nm for Yb:KGW. The results reported in Table 2 clearly show that the gain at 997 nm is much higher for Yb:KGW than for Yb:KYW at 1000 nm. Consequently, to limit the line competition, we prefer Yb:KYW, even if its spectroscopic properties are slightly lower at 981 nm.

Table 1. Comparison of the Spectroscopic Properties at 981 nm for Yb:KGW and Yb:KYW

	Yb:KYW	Yb:KGW
Effective emission cross section σ_{el}(981 nm)	13.4×10^{-20} cm^2	15×10^{-20} cm^2
Effective absorption cross section σ_{al}(981 nm)	11.5×10^{-20} cm^2	11.6×10^{-20} cm^2
Lifetime τ	440 μs	438 μs

3. CHOICE OF THE Yb:KYW ABSORPTION

The basic principle for the intracavity pumping of Yb:KYW is reported in Fig. 2. For the pumping, we chose a Nd : YVO_4 laser pumped by a laser diode at 808 nm. This laser operated at 914 nm is referred to as the pump laser in the rest of the paper. 914 nm is far from the absorption band of Yb:KYW, which is typically between 930 and 981 nm. However, the small absorption coefficient will be compensated by the high value of the intracavity power at 914 nm. The Yb:KYW crystal is introduced in the cavity of the 914 nm laser, which is a high-finesse resonator. For the sake of simplicity, the cavities at 981 and 914 nm are superimposed, thanks to specific coatings on the mirrors.

In an intracavity pumping configuration, the choice of the crystal absorption is critical: if it is too high, it increases the threshold of the pump laser; if it is too low, it reduces the output power. Indeed, the optimum absorption is strongly related to the optimum output coupling for the pump laser as previously mentioned for intracavity pumped lasers [18]. To specify the Yb:KYW crystal (i.e., length and doping concentration), one has to study the pump laser first. The experimental setup for the pump Nd : YVO_4 laser is presented in Fig. 3.

We used a laser diode emitting at 808 nm coupled into a 100 μm core diameter fiber with a numerical aperture of 0.22. This diode provides up to 25 W of unpolarized emission. The fiber output is imaged with two identical doublets (60 mm focal length) into the Nd : YVO_4 crystal with a waist radius of 50 μm. The 5 mm long, a-cut 0.1% doped Nd : YVO_4 crystal is antireflection (AR) coated at 914 and 981 nm to reduce the intrinsic losses of the cavity. It was oriented with its c axis perpendicular to the plan of the cavity such that laser emission at 914 nm will be linearly polarized perpendicularly to this plan. It is also AR coated at 1064 nm to prevent laser oscillation between the two facets of the crystal. The first three mirrors of the cavity (M_1, M_2, and M_3) are highly reflective at both 914 and 981 nm and highly transmissive at 1064 nm, once again to prevent the parasitic oscillation of the high gain transition line in the Nd : YVO_4. The last mirror of the cavity (M_4) is the output coupler for the 981 nm emission, but still highly reflecting at 914 nm. Different output couplers are used in this

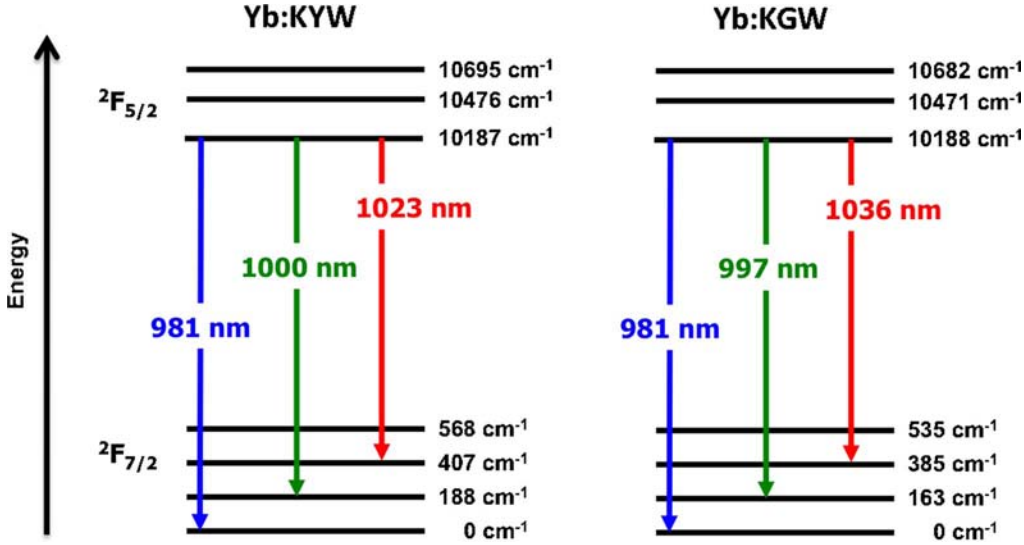

Fig. 1. (Color online) Energy levels in Yb:KYW and Yb:KGW and associated emission wavelengths.

Table 2. Comparison of the Gain Cross Section at 1000 nm and 997 nm for Yb:KYW and Yb:KGW, Respectively, for a Transparency at 981 nm

	Yb:KYW	Yb:KGW
x_{tr} at 981 nm transparency	0.46	0.44
Wavelength considered	1000 nm	997 nm
Effective emission cross section σ_{el}	5.1×10^{-20} cm^2	8.3×10^{-20} cm^2
Effective absorption cross section σ_{al}	1.6×10^{-20} cm^2	1.8×10^{-20} cm^2
$\sigma_g(x_{tr})$ (at 1000 or 997 nm)	1.5×10^{-20} cm^2	2.6×10^{-20} cm^2

[a]The cross sections come from [13,14].

study with a transmission between 20% and 70% at 981 nm. The second waist of the cavity (between M_3 and M_4), has a size of 40 μm (radius) and is used to introduce the AR-coated (at 981 and 914 nm) Yb:KYW crystal.

Knowing all the parameters of the laser, we developed a theoretical simulation to find the optimum output coupling at 914 nm of this laser. For the calculations, we used the formalism described in [19]. Figure 4 gives the computed output power versus the transmission of the output coupler. It shows an optimum coupling around 7% at 914 nm. Indeed, the absorption of the Yb:KYW crystal can be considered as a coupling outside the cavity. The crystal absorption is then equivalent to the transmission of an output coupler, and the absorbed power at 914 nm is equivalent to the output power at 914 nm. For the experiment, we had at our disposal a 2.5 mm 2% doped Yb:KYW (corresponding to a doping concentration of 1.27×10^{20} atoms per cm^2).The crystal was cut along the Ng axis in order to benefit from the strong emission at 981 nm for a polarization along the Nm axis. Following the spectral shape of the effective absorption cross section σ_{ap} [13], we can estimate that $\sigma_{ap/Nm}(914\text{ nm}) = 0.4\times10^{-20}$ cm^2 for a polarization parallel to the Nm axis and $\sigma_{ap/Np}(914\text{ nm}) = 0.2\times10^{-20}$ cm^2 for a polarization parallel to the Np axis. This leads to a double pass absorption of 23.8% for the Nm axis and 12.2% for the Np axis, in small signal, i.e., without saturation of absorption. As shown in Fig. 4, the absorption parallel to the Np axis is relatively close the optimum, whereas the absorption parallel to the Nm axis is too high. As the Nd : YVO_4 laser emits a linearly polarized beam at 914 nm, the crystal must be oriented such that its Np axis is parallel to the Nd : YVO_4 linear polarization. This was confirmed experimentally: with the Yb:KYW Np axis perpendicular to the Nd : YVO_4 polarization, the laser at 914 nm was very close to the threshold at the maximum of pump power (23 W at 808 nm). For the other orientation (Np axis parallel), the pump power at threshold was reduced to less than 8 W.

The absorption of the Yb:KYW may also depend on the laser regime: if the output coupling at 981 nm is high, the population inversion needs to be significant. It is correlated with a

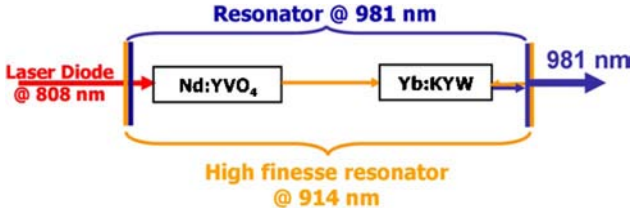

Fig. 2. (Color online) Basic principle for Yb:KYW intracavity pumping.

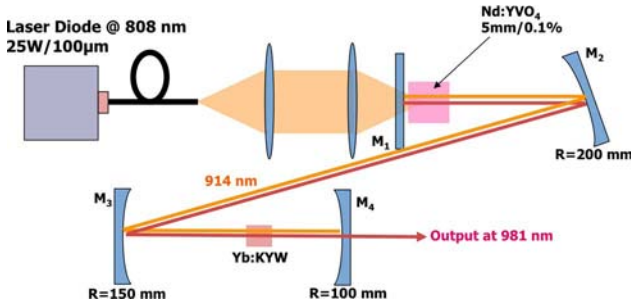

Fig. 3. (Color online) Experimental setup for laser operation at 981 nm under intracavity pumping. M_1, M_2, and M_3 are highly reflective mirrors at both 914 and 981 nm and highly transmissive at 1064 nm. M_1, is the output coupler at 981 nm, and it is also highly reflective at 914 nm.

depletion of the ground state and, hence, to a saturation of the absorption at 914 nm. In this case, the small signal absorption is not the relevant parameter to choose the appropriate Yb:KYW. One has to choose a crystal with a small signal absorption higher than the optimum value given in Fig. 4. Conversely, if the laser operates in a highly reflective cavity at 981 nm, as it is the case for intracavity SHG, the ground state depletion is limited, and one has to chose a small signal absorption close to the optimum value.

4. CHOICE OF THE MIRROR TRANSMISSION: EFFECT OF THE LINE COMPETITION

In this section, we consider the line competition between the 981 nm line and the closest lines at 1000 and 1023 nm existing in Yb:KYW. Even if the emission spectrum is continuous in Yb:KYW, we consider only the emission at these peak wavelengths where the laser will tend to oscillate predominantly. As shown in Fig. 1, these transitions start from the same emitting level, but the lower level is different. It is the ground state for the transition at 981 nm, and it corresponds to higher energy levels for the transitions at 1000 and 1023 nm.

We focus the study on the oscillation threshold at the different wavelengths as a function of the pump power at 914 nm. In our case of intracavity pumping, the pump power is the intracavity power P_{914} at 914 nm. From the Fig. 4 (by dividing the output power by the transmission), we can estimate that the intracavity power at 914 nm can reach values on the order of 100 W at maximum pump power. This order of

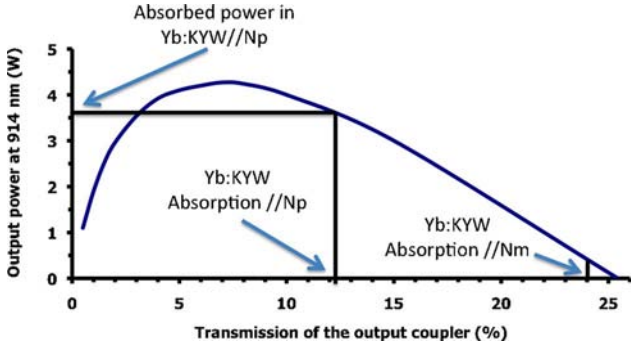

Fig. 4. (Color online) Computed optimum output coupling for the Nd : YVO_4 laser pumped at 23 W. The passive losses are fixed to 3% at 914 nm to take the different mirrors into account. The absorptions of our Yb:KYW are given in double pass.

magnitude was also experimentally confirmed by the measurement of the power leaking through the mirror M3.

In order to calculate the small signal gain coefficient, different approximations can be done. The Rayleigh length in the Yb:KYW is approximately 10 mm, which means that we can assume a constant beam size for the pump and the signal in the crystal (having a length of 2.5 mm). As the Yb:KYW crystal introduces relatively low losses and is pumped on the both sides in the 914 nm linear cavity, we can assume that the intracavity power P_{914} is constant in each point of the crystal. For the calculations, we used the rate equations and the gain coefficient given in [19]. We assume that the effective emission cross section at 914 nm is null for Yb:KYW and that the transverse profile of the laser beam at 914 nm has a Gaussian shape. For a very small laser signal (meaning that the laser intensity can be neglected in the calculation), we can write the small signal gain coefficient at the wavelength λ (981, 1000, or 1023 nm) as

$$g_0(r,\lambda,P_{914}) = n_t \frac{\sigma_{\mathrm{el}}(\lambda)\cdot\sigma_{\mathrm{ap}}\frac{2P_{914}}{h\nu_{914}\pi w_{914}^2}\exp\left(-\frac{2r^2}{w_{914}^2}\right)-\frac{\sigma_{\mathrm{al}}(\lambda)}{\tau}}{\sigma_{\mathrm{ap}}\frac{2P_{914}}{h\nu_{914}\pi w_{914}^2}\exp\left(-\frac{2r^2}{w_{914}^2}\right)+\frac{1}{\tau}}, \quad (2)$$

where ν_{914} is the frequency associated to the wavelength 914 nm and $w_{914} = 40\ \mu$m is the 914 nm beam size.

Assuming that the beam size is also constant at the wavelength λ, with a radius denoted w_λ, the small signal gain G_0 can be expressed as a function of the intracavity power at 914 nm and the wavelength λ:

$$G_0(\lambda,P_{914}) = \mathrm{Exp}\left(l\cdot\int_0^r \frac{4g_0(r,\lambda,P_{914})}{w_\lambda^2}\cdot\exp\left(-\frac{2r^2}{w_\lambda^2}\right)r\mathrm{d}r\right), \quad (3)$$

where l is the length of the Yb:KYW and r_c is the crystal radius (1.5 mm in our case).

Figure 5 shows the small signal gain versus the intracavity pump power at 914 nm. The shapes are very different versus the wavelength. The gain starts to be very close to 0 at 981 nm (strong signal absorption) and becomes high for large intracavity pump powers. This behavior can be related to the three-level nature of this transition coupled with a strong effective emission cross section. Conversely, the lower levels of the transitions at 1000 and 1023 nm are less thermally populated, involving higher gain at low pump power, but the smaller effective emission cross section at these wavelengths limits the gain value at high pump power levels.

The oscillation threshold is also related to the cavity losses. As the transmission of the cavity mirrors varies as a function of the wavelength, we introduce $T(\lambda)$, the transmission of the "cold" cavity (i.e., without the gain media) after one round trip. This quantity results from the knowledge of the transmission curves of the cavity mirrors and the passive losses (denoted as L and should be independent of the wavelength). Consequently,

$$T(\lambda) = T_1(\lambda) + T_2(\lambda) + T_3(\lambda) + T_4(\lambda) + L, \quad (4)$$

where T_1, T_2, T_3, and T_4 are the transmissions of the mirrors M_1, M_2, M_3, and M_4, respectively.

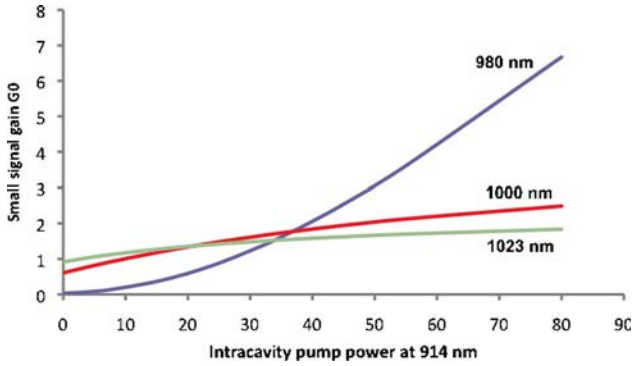

Fig. 5. (Color online) Small signal gain calculated at 981, 1000, and 1023 nm as a function of the intracavity pump power at 914 nm. For the three wavelengths, the beam size w_λ is equal to 50 μm.

Moreover, at a fixed intracavity power P_{914}, we introduce the threshold cavity transmission $T_{\mathrm{th}}(\lambda,P_{914})$ corresponding to the value of the cavity transmission needed to reach the oscillation threshold at the considered wavelength. Following this definition, T_{th} is related to the small signal gain by

$$T_{\mathrm{th}}(\lambda,P_{914}) = 1 - \frac{1}{G_0^2(\lambda,P_{914})}. \quad (5)$$

The benefit to using this quantity is that the discussion can be concentrated on the transmission of the mirrors. As it is shown in the end of this section, the use of T_{th} enables one to deduce the mirror transmission values needed for laser oscillation at 981 nm very easily.

Figure 6 presents the threshold cavity transmission T_{th} at the three wavelengths of interest (981, 1000, and 1023 nm) for different intracavity powers at 914 nm. For better legibility, lines between points have been plotted. A value of zero for T_{th} means that the laser must operate without losses to reach the oscillation threshold: this value is obtained when the pump power is equal to the pump transparency (i.e., G_0 is equal to unity). Conversely, a negative value for T_{th} would correspond an absorbant laser medium, where the population inversion is not high enough to reach the transparency (i.e., G_0 is less than unity). A negative value has no physical significance (and is not represented on the Fig. 6); it just indicates that the oscillation threshold cannot be reached.

For low powers at 914 nm (8 W), the oscillation threshold can be reached only at 1023 nm as this transition requires only a small amount of population inversion to reach the transparency. The lower level of the laser transition being more populated at 1000 nm, the pump power required to reach the transparency is higher (typically between 8 and 16 W). This effect is even more pronounced at 981 nm since a pump power between 24 and 32 W is needed. Thanks to Fig. 6, we can also observe the evolution of the cavity threshold transmission when the pump power increases for the three wavelengths. It is clear that T_{th} increases at a much smaller rate at 1023 than at 1000 than at 981 nm. This is due to the effective emission cross section increasing from 1023 to 981 nm: once the transparency is reached, the gain in the medium is very high at 981 nm (as shown in Fig. 5). As an example, T_{th} can reach a value of 97.7% at 981 nm for an intracavity pump power of 80 W. This corresponds to a large small signal gain of $G_0 = 6.6$. Consequently, the shape of T_{th} versus the wavelength is modified following the intracavity pump power. At low intracavity power, it has a maximum at 1023 nm. Next, it peaks at

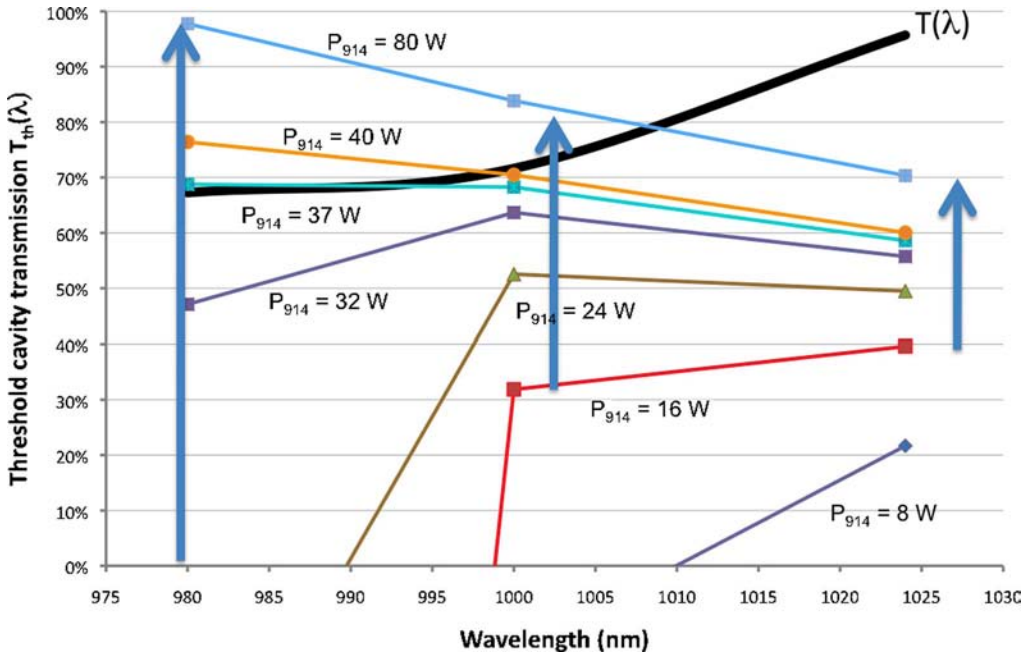

Fig. 6. (Color online) Threshold cavity transmission T_{th} at the three wavelengths of interest (981, 1000, and 1023 nm) for different intracavity powers at 914 nm. The arrows show the moving of T_{th} when the intracavity power increases.

1000 nm for intracavity power between 16 and 32 W. Finally, it has a maximum at 981 nm for higher values of P_{914}.

In order to know which wavelength can reach the threshold first, one has to consider the cavity transmission curve $T(\lambda)$, as defined earlier. One example is given in Fig. 6 for a set of mirrors having a lower transmission at 981 nm (the passive losses are estimated to be 1%). At a given pump power, the oscillation threshold is reached if $T_{\mathrm{th}}(\lambda, P_{914}) = T(\lambda)$. As an example, Fig. 6 shows that the oscillation threshold is reached close to 37 W for the 981 nm wavelength and at higher powers at 1000 and 1023 nm.

To understand the line competition, one has to know which wavelength reaches the oscillation threshold first. We assume that the intracavity pump power varies continuously from zero to its maximum value when the laser is switched on. Given the shapes of $T_{\mathrm{th}}(\lambda, P_{914})$ and the way $T_{\mathrm{th}}(\lambda, P_{914})$ increases when P_{914} increases, it is clear that the first wavelength to reach the oscillation threshold is 981 nm in the particular case of $T(\lambda)$ presented in Fig. 6. Once the oscillation threshold is reached, the gain is clamped at its value at threshold. This means that $T_{\mathrm{th}}(\lambda, P_{914})$ does not move once the laser is running, as this quantity is related to the gain by Eq. (5). Consequently, the oscillation threshold can never be reached at 1000 and 1023 nm. In this case, we observed a laser oscillation at 981 nm only. This behavior was experimentally confirmed. Figure 7 presents the output power at 981 nm versus the pump power of the Nd : YVO_4 laser. An output power of 1 W has been achieved in this configuration.

We also tested other output couplers (M_4) having lower transmissions and other spectral shapes. Figure 8 gives the transmission cavity curve in two cases [$T_1(\lambda)$ and $T_2(\lambda)$]. Even if $T_{\mathrm{th}}(\lambda, P_{914})$ is given for fixed values of P_{914} in Fig. 8 (for the sake of simplicity), we can estimate the oscillation threshold and deduce the wavelength that reaches the threshold first. The method is to consider the slope of $T_{\mathrm{th}}(\lambda, P_{914})$ with respect to the slope of the transmission cavity curves. Let us study the curve $T_{\mathrm{th}}(\lambda, 32\ \mathrm{W})$ with respect to $T_1(\lambda)$ as an example: the wavelengths 981 and 1000 nm seem to be above the oscillation threshold. However, one has to consider which wavelength reaches the threshold first. As the slope of $T_{\mathrm{th}}(\lambda, 32\ \mathrm{W})$ between 981 and 1000 nm is larger than the slope of $T_1(\lambda)$, it is also the case for the slope of $T_{\mathrm{th}}(\lambda, P_{914})$ for lower values of pump power [see the evolution of $T_{\mathrm{th}}(\lambda, P_{914})$ in Fig. 8]. Consequently, when the laser reaches the threshold at 1000 nm (for a pump power of approximately 30 W), the laser is below the threshold at 981 nm. Finally, the laser oscillates only at 1000 nm for the transmission cavity $T_1(\lambda)$.

The same demonstration can be carried out for the transmission cavity $T_2(\lambda)$: in this case, the first wavelength appearing is 1023 nm at a pump power of approximately 10 W. Both cases were experimentally confirmed [9].

Hence, the choice of the mirror transmission is critical in order to operate the laser at 981 nm. Two rules can be set following this study: first, a high output coupling promotes the laser oscillation at 981 nm. For a flat transmission curve $T(\lambda)$, this will correspond to a value of approximately $T(\lambda) = 70\%$ (see Fig. 9). Second, 981 nm can be favored if we can control the shape of the transmission curve. For a laser oscillation at 981 nm in a highly reflective cavity at 981 nm (necessary for SHG), the cavity transmission needs to be higher than 65% at 1000 nm and higher than 55% at 1023 nm (Fig. 9). It is worth noting that these transmissions are lower than the maximum

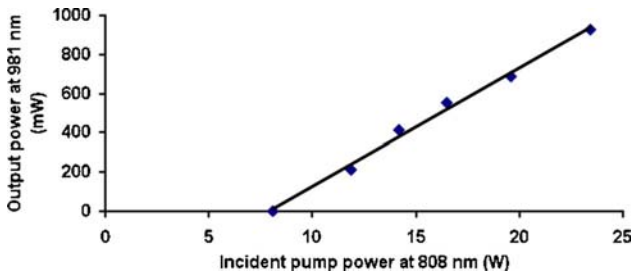

Fig. 7. (Color online) Laser emission at 981 nm as a function of the pump power for the Nd : YVO_4 laser (at 808 nm).

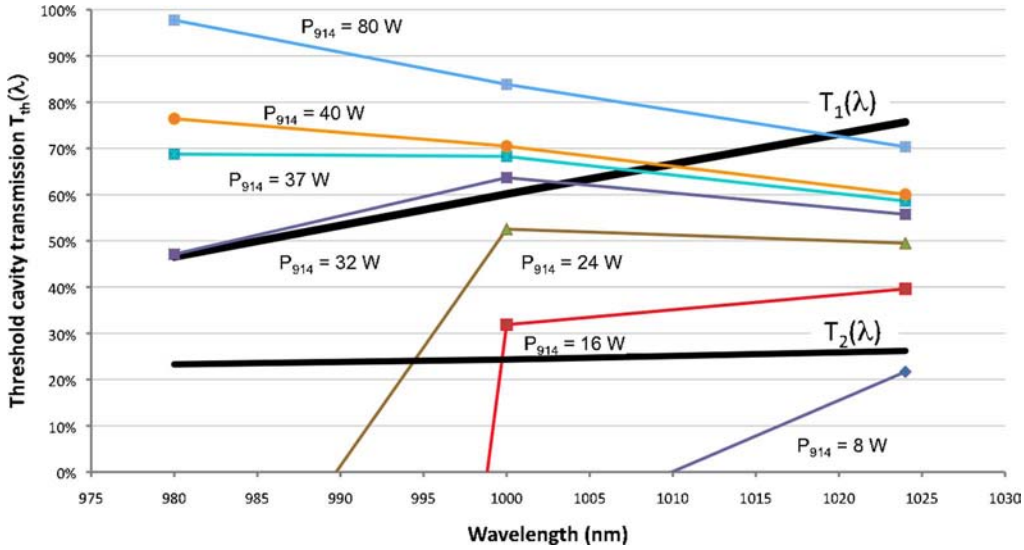

Fig. 8. (Color online) Threshold cavity transmission T_{th} and cavity transmission in two cases (T_1 and T_2) corresponding to different mirrors M_4.

values of T_{th} at the considered wavelengths. A rough analysis would lead one to choose dichroïc mirrors introducing losses at 1000 and 1023 nm that are higher than the maximum gain. This means $T > T_{\text{th}}$ and corresponds to a transmission higher than 85% at 1000 nm and higher than 70% at 1023 nm. Hence, this analysis of the line competition allows one to reduce the transmission requirements on the cavity mirrors.

5. EFFECT OF THE TEMPERATURE ON THE LINE COMPETITION

As mentioned in [9], when we used an output coupler leading to the transmission curve $T_1(\lambda)$ (described in Fig. 8), we observed a laser oscillation at 1000 nm at room temperature. However, we observed a wavelength switch at 981 nm when the temperature reached 360 K and a laser operation at 981 nm for higher temperatures. The purpose of this section is to explain how these two transitions are temperature dependent and how they affect the line competition.

The effective absorption cross section is related to the temperature T by the fractional population of the different sublevels:

$$\sigma_{\text{al}}(T) = \sigma_{\text{al}}(T_0)\frac{f_a(T)}{f_a(T_0)} \tag{6}$$

with the fractional population

$$f_a(T) = \frac{\exp\left(-\frac{E_l}{kT}\right)}{\sum_i \exp\left(-\frac{E_i}{kT}\right)}, \tag{7}$$

where E_1 is the energy level concerned by the transition, E_i represents any energy level of the ground state manifold (see Fig. 1), k is the Boltzmann constant, and T_0 is the reference temperature (300 K in our case).

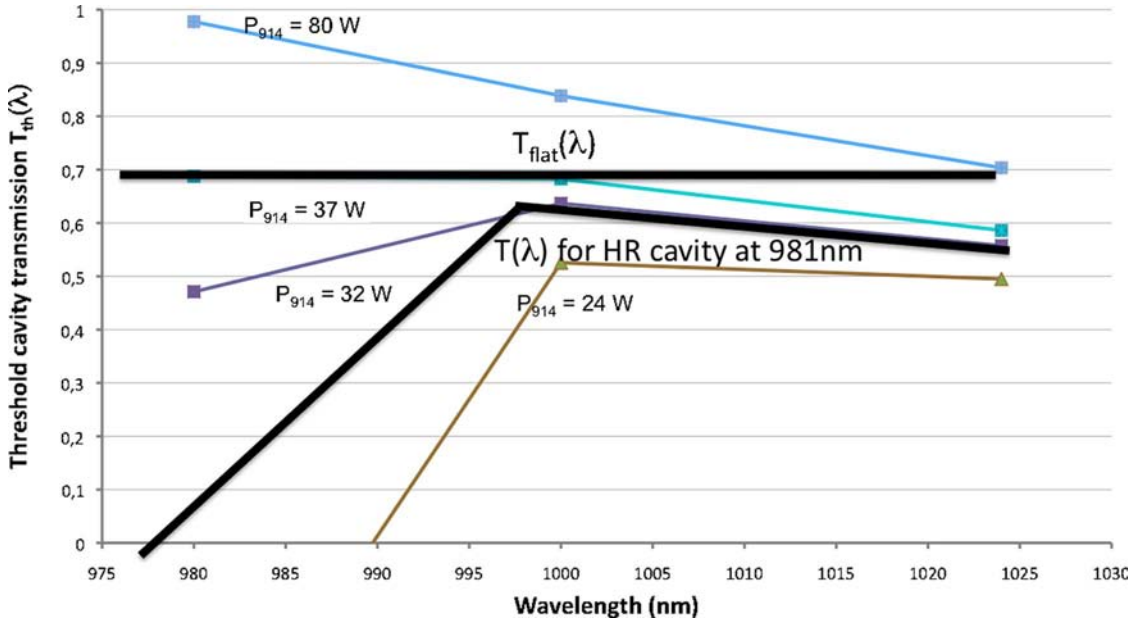

Fig. 9. (Color online) Shape of cavity transmission for laser action at 981 nm in two cases. Case 1 has a high output coupling and a flat transmission curve ($T_{\text{flat}}(\lambda)$). Case 2 has a highly reflective cavity ($T(\lambda)$ for HR cavity at 981 nm).

In the same way, the effective emission cross section can be expressed versus the temperature:

$$\sigma_{\mathrm{el}}(T) = \sigma_{\mathrm{el}}(T_0)\frac{f_e(T)}{f_e(T_0)} \tag{8}$$

with the fractional population

$$f_e(T) = \frac{\exp\left(-\frac{E_2}{kT}\right)}{\sum_j \exp\left(-\frac{E_j}{kT}\right)}, \tag{9}$$

where E_2 is the emitting level and E_j represents any energy level of the excited state manifold.

Using the Eqs. (6)–(9), we plot the relative variation of the cross sections versus the temperature in Fig. 10. At 981 nm, both emission and effective absorption cross sections decrease versus temperature. This is due to the depletion of the ground state and the emitting level by the Boltzmann law. The effective emission cross section at 1000 nm follows the same behavior, as it is related to the same emitting level. Conversely, the effective absorption cross section at 1000 nm increases versus temperature. This is due to the thermal population of the lower level. Figure 10 clearly highlights the difference between a pure three-level transition (981 nm) and the quasi-three-level transition (1000 nm).

Equations (2) and (3) can be rewritten with a dependency of temperature, including the expressions of σ_{el} and σ_{al} versus temperature. In Eq. (2), two other parameters can vary with the temperature: the effective absorption cross section σ_{ap} and, consequently, the intracavity power at 914 nm: P_{914}. Following the absorption value of our Yb:KYW and by the help of Fig. 4, it is clear that P_{914} increases if the absorption decreases. Consequently, the product $\sigma_{\mathrm{ap}}P_{914}$ [as is stated in Eq. (2)] will be much less sensitive to temperature than the cross sections. It is supposed to be constant to simplify the following calculations.

With the knowledge of the cross sections variation versus temperature, it is possible to calculate the threshold cavity transmission as a function of temperature. This was reported in Fig. 11 for an intracavity pump power of 32 W at 914 nm

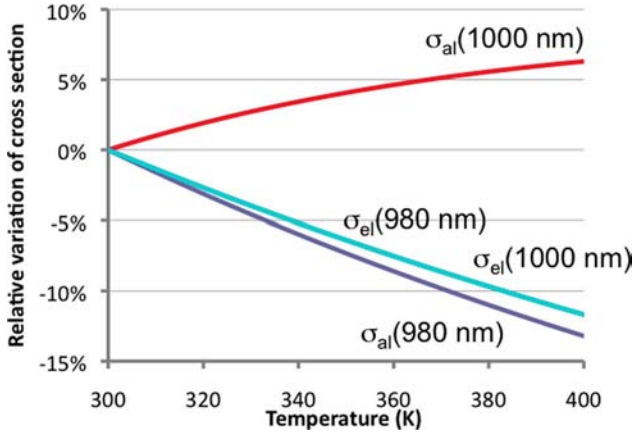

Fig. 10. (Color online) Relative variation of cross sections at 981 and 1000 nm versus the temperature. The references are the cross sections at 300 K. The curves for the effective emission cross sections are superimposed.

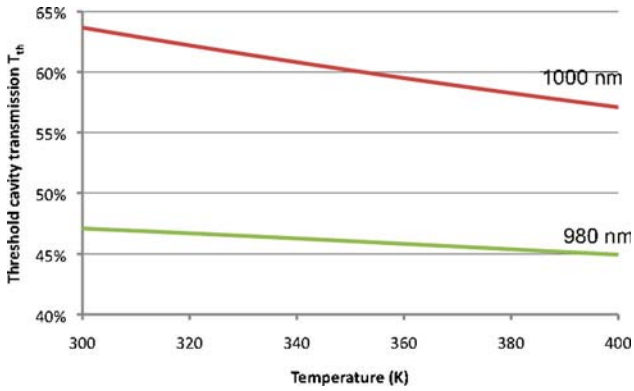

Fig. 11. (Color online) Threshold cavity transmission versus temperature at 981 and 1000 nm for an intracavity pump power of 32 W at 914 nm.

(close to the oscillation threshold for the cavity transmission T_1). In both cases (981 and 1000 nm), the threshold cavity transmission decreases with the temperature. This is of course related to the gain decrease with the temperature, and means that the pump power needs to be higher in order to reach the oscillation threshold. Because of the quasi-three-level nature of the transition at 1000 nm, the decrease of T_{th} is more pronounced at 1000 than at 981 nm.

Finally, we can use the same approach as the one presented in the previous sections to understand the line competition versus temperature. Figure 12 gives the threshold transmission T_{th} for three temperatures (300, 360, and 400 K) and its position with respect to the cavity transmission $T_1(\lambda)$. At 300 K, the first wavelength reaching the oscillation threshold (when the pump power increases) is 1000 nm for a pump power slightly lower than 32 W, as explained in Section 4. At 360 K, the slope of T_{th} is exactly the same as the slope of $T_1(\lambda)$, which means that both wavelengths reach the oscillation threshold for the same pump power (32 W). At $T = 400$ K, the slope of T_{th} is lower than the slope of $T_1(\lambda)$. Hence, the oscillation threshold will be reached at 981 nm first for a pump power slightly higher than 32 W. Consequently, this theoretical analysis is in agreement with the experimental behavior of the laser: at a temperature higher than 360 K, the three-level transition at 981 nm is promoted.

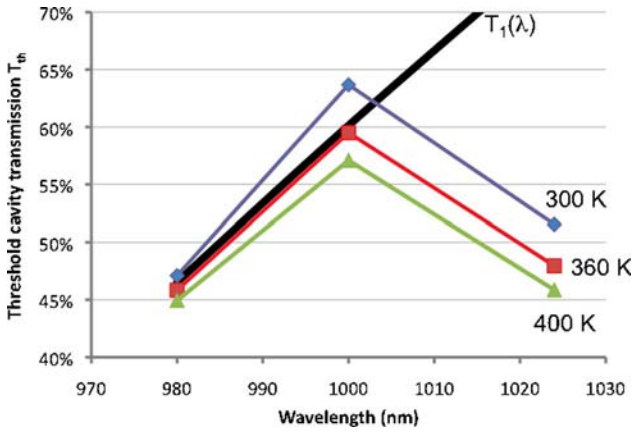

Fig. 12. (Color online) Threshold cavity transmission T_{th} and cavity transmission (T_1) for three temperatures: 300, 360, and 400 K for an intracavity pump power of 32 W at 914 nm.

6. CONCLUSION

This paper has presented a theoretical analysis of an intracavity-pumped Yb-doped KYW operating at 981 nm. It gives some guidelines to develop a bulk laser on this three-level transition. It demonstrates that Yb:KYW is more suitable than Yb:KGW because of a less pronounced line competition with the closest quasi-three-level line at 1000 nm.

Then it explained that the crystal absorption needs to correspond to the optimum output coupling for the pump laser in an intracavity pumping configuration. In our case (pumping at 914 nm with a Nd : YVO_4 laser, itself pumped at 808 nm), it corresponds to a double pass absorption of 7%. This order of magnitude can be easily found in standard commercial Yb:KYW (Ng cut 2.5 mm long 2% doped Yb:KYW). In Section 4, we introduced a simple and original method to explain the line competition occurring in Yb:KYW between 981 nm and the quasi-three-level lines at 1000 and 1023 nm. This method is based on the threshold cavity transmission, a quantity related to the small signal gain of the Yb:KYW. This method enables one to explain the laser behavior experimentally observed: the emission wavelength dependence following the output mirror transmission and its spectral shape. It highlights two ways to promote the 981 nm transition. First, an output coupler with a large transmission at 981 nm will favor the 981 nm emission since the gain on this transition is much higher than the gain at 1000 and 1023 nm. Under these conditions (output coupler with a transmission of 67%), we achieved an output power of 1 W at 981 nm for a pump power at 808 nm of 22 W. Second, the laser oscillation at 981 nm only can be achieved thanks to the spectral selectivity of the cavity mirrors, which allows one to operate in a highly reflective cavity at 981 nm in order to realize intracavity SHG at 490.5 nm. Our analysis of the line competition shows that the transmission requirements at 1000 and 1023 nm can be relaxed compared to a rough analysis setting that the cavity losses should be higher than the maximum gain at this wavelength. Hence, the cavity transmission should be 65% at 1000 nm instead of 85% and 50% at 1023 nm instead of 70%.

Finally, we propose for the first time an analysis of the line competition versus the temperature. The thermal population of the different energy levels, associated with the different nature of the transitions, explain why the three-level line at 981 nm is favored when the temperature increases. Our analysis is in agreement with the wavelength switch between 1000 and 981 nm experimentally observed when the temperature reached 360 K.

The results and analysis obtained here can contribute to the design of a microchip laser integrating the intracavity pumping, the highly reflective cavity at 981 nm, and the nonlinear crystal for SHG at 490.5 nm. From a more general point of view, the simplicity of the threshold cavity transmission method to understand the line competition could be useful for other lasers, such as Nd lasers operating on the three-level transition at 880 nm [20].

REFERENCES

1. O. G. Okhotnikov, L. A. Gomes, N. Xiang, T. Jouhti, A. K. Chin, R. Singh, and A. B. Grudinin, "981 nm picosecond fiber laser," IEEE Photon. Technol. Lett. **15**, 1519–1521 (2003).
2. K. H. Ylä-Jarkko, R. Selvas, D. B. S. Soh, J. K. Sahu, C. A. Codemard, J. Nilsson, S. A. Alam, and A. B. Grudinin, "A 3.5 W 977 nm cladding pumped jacketed air clad ytterbium doped fiber laser," in *Advanced Solid-State Photonics*, J. Zayhowski, ed., Vol. 83 of OSA Trends Optics Photonics (Optical Society of America, 2003), paper 103.
3. J. Boullet, Y. Zaouter, R. Desmarchelier, M. Cazaux, F. Salin, J. Saby, R. Bello-Doua, and E. Cormier, "High power ytterbium-doped rod-type three- level photonic crystal fiber laser," Opt. Express **16**, 17891–17902 (2008).
4. F. Röser, C. Jauregui, J. Limpert, and A. Tünnermann, "94 W 981 nm high brightness Yb-doped fiber laser," Opt. Express **16**, 17310–17318 (2008).
5. D. B. S. Soh, C. Codemard, S. Wang, J. Nilsson, J. K. Sahu, F. Laurell, V. Philippov, Y. Jeong, C. Alegria, and S. Baek, "A 981 nm Yb-doped fiber MOPA source and its frequency doubling," IEEE Photon. Technol. Lett. **16**, 1032–1034 (2004).
6. A. Bouchier, G. Lucas-Leclin, and P. Georges, "Frequency doubling of an efficient continuous wave single-mode Yb-doped fiber laser at 978 nm in a periodically-poled MgO:LiNbO3 waveguide," Opt. Express **13**, 6974–6979 (2005).
7. M. Castaing, F. Balembois, P. Georges, T. Georges, K. Schaffers, and J. Tassano, "Diode-pumped Nd:YVO4/Yb:S-FAP laser emitting at 985 and 492.5 nm," Opt. Lett. **33**, 1234–1236 (2008).
8. A. Bouchier, G. Lucas-Leclin, F. Balembois, and P. Georges, "Intense laser emission at 981 nm in an Ytterbium-doped $KY(WO_4)_2$ crystal," in *Advanced Solid-State Photonics (TOPS)*, C. Denman and I. Sorokina, eds., Vol. 98 of OSA Trends Optics Photonics (Optical Society of America, 2005), paper TuB5.
9. M. Castaing, F. Balembois, P. Georges, and T. Georges, "Diode-pumped Yb :KYW laser emitting at 981 nm by intracavity pumping," Proc. SPIE **7193**, 71930J (2009)
10. Y. F. Lü, X. H. Zhang, J. Xia, R. Chen, G. Y. Jin, J. G. Wang, C. L. Li, and Z. Y. Ma, "981 nm Yb:KYW laser intracavity pumped at 912 nm and frequency-doubling for an emission at 490.5 nm," Laser Phys. Lett. **7**, 343–346 (2010).
11. N. V. Kuleshov, A. Alagatsky, A. V. Podlipensky, V. P. Mikhailov, and G. Huber, "Pulsed laser operation of Yb-doped $KY(WO_4)_2$ and $KGd(WO_4)_2$," Opt. Lett. **22**, 1317–1319 (1997).
12. S. A. Payne, L. D. DeLoach, L. K. Smith, W. L. Kway, J. B. Tassano, W. F. Krupke, B. H. T. Chai, and G. Loutts, "Ytterbium-doped apatite-structure crystals: a new class of laser materials," J. Appl. Phys. **76**, 497–503 (1994).
13. A. A. Lagatsky, N. V. Kuleshov, and V. P. Mikhailov, "Diode-pumped CW lasing of Yb:KYW and Yb:KGW," Opt. Commun. **165**, 71–75 (1999).
14. Eksma Optics, "Yb:KGW and Yb:KYW crystals," http://www.eksmaoptics.com/en/p/yb-kgw-and-yb-kyw-crystals-498?t=brochures.
15. S. Bjurshagen, J. E. Hellström, V. Pasiskevicius, M. Cinta Pujol, M. Aguiló, and F. Díaz, "Fluorescence dynamics and rate equation analysis in Er3+ and Yb3+ doped double tungstates," Appl. Opt. **45**, 4715–4725 (2006).
16. A. A. Demidovich, A. N. Kuzmin, G. I. Ryabtsev, M. B. Danailov, W. Strek, and A. N. Titov, "Influence of Yb concentration on Yb:KYW laser properties," J. Alloys Compd. **300–301**, 238–241 (2000).
17. N. V. Kuleshov, A. A. Lagatsky, A. V. Podlipensky, V. P. Mikhailov, E. Heumann, A. Diening, and G. Huber, "Highly efficient CW and pulsed lasing of Yb doped tungstates," in *Advanced Solid State Lasers*, C. Pollock and W. Bosenberg, eds., Vol. 10 of OSA Trends in Optics and Photonics Series (Optical Society of America, 1997), paper SC3.
18. S. So, J. I. Mackenzie, D. P. Shepherd, W. A. Clarkson, J. G. Betterton, E. K. Gorton, and J. A. C. Terry, "Intra-cavity side-pumped Ho:YAG laser," Opt. Express **14**, 10481–10487 (2006).
19. F. Augé, F. Druon, F. Balembois, P. Georges, A. Brun, F. Mougel, G. Aka, and D. Vivien, "Theoretical and experimental investigations of a diode-pumped quasi-three level laser: the Yb^{3+}-doped $Ca_4GdO(BO_3)_3$ (Yb:GdCOB) laser," IEEE J. Quantum Electron. **36**, 598–606 (2000).
20. M. Castaing, E. Hérault, F. Balembois, P. Georges, C. Varona, P. Loiseau, and G. Aka, "Diode-pumped Nd:YAG laser emitting at 899 nm and below," Opt. Lett. **32**, 799–801 (2007).